PAPER

Breathing impure plasmas

IOP Publishing Plasma Physics and Controlled Fusion
Plasma Phys. Control. Fusion **66** (2024) 075018 (10pp) https://doi.org/10.1088/1361-6587/ad5105

Breathing impure plasmas

Y Kosuga[1,*], J Bourgeois[2,3], M Lesur[4] and I Oyama[3]

[1] Research Institute for Applied Mechanics, Kyushu University, Kasuga, Fukuoka 816-8580, Japan
[2] Ecole Polytechnique, Institut Polytechnique de Paris, 91128 Palaiseau, France
[3] Interdisciplinary Graduate School of Engineering Sciences, Kyushu University, Kasuga, Fukuoka 816-8580, Japan
[4] Universite de Lorraine, CNRS, Institut Jean Lamour, UMR 7198, F-54000 Nancy, France

E-mail: kosuga@riam.kyushu-u.ac.jp

Received 18 January 2024, revised 9 May 2024
Accepted for publication 28 May 2024
Published 6 June 2024

Abstract

A theory is presented to describe fluctuation dynamics in magnetized plasmas with impurities. In particular, it is shown that impurities can significantly facilitate an abrupt transient increase of fluctuation amplitude. To demonstrate this, a fluid model is derived to describe how impurities enter fluctuation dynamics. At the linear level, a wave similar to a drift wave can be excited in the presence of impurities. The nonlinear dynamics of this wave is formulated via modulational analysis, and it is demonstrated that drift waves with impurities can develop into a breather, a nonlinear wave that exhibits transient increase of amplitude. Our model indicates that nonlinear breathers become easier to be excited as impurity concentration increases. Breathers transiently increase fluctuation amplitude, and hence may be important to expel impurities. Implications on basic experiments and magnetic fusion are discussed as well.

Keywords: impurity, drift wave, nonlinear evolution, nonlinear breather

1. Introduction

Turbulence and transport are important issues for magnetically confined plasmas. While progress has been made, a critical issue related to these problems is to understand the overall particle balance in fusion plasmas [1]. Namely, fusion plasmas consist of main fuel ions and impurities. Impurities arise from fusion product and/or plasma-wall interaction, and they cause fuel dilution and radiation. We need to avoid accumulation of impurities, and this poses a challenge: We need to expel undesired components in plasmas without, or at least by minimizing, confinement degradation of fuel particles and bulk plasma energy.

One approach to reconcile good confinement of bulk plasma particles and energy and poor confinement of undesired elements may be to invoke transport interference. Turbulent transport in fusion plasmas is not so simple in that particles, momentum and heat are not expelled altogether. In some cases, relaxation in one transport channel leads to the excitation of secondary profile in another transport channel. To give specific examples, transport of heat often leads to non-diffusive transport of momentum, and as a result intrinsic rotation arises in toroidal plasmas [2, 3]. Another is a particle pinch, where transport of heat and/or momentum leads to the peaking of density [4, 5]. By invoking this property, we may be able to identify relevant fluctuations to expel impurities while peaking fuel density/energy. Indeed, state-of-the-art gyrokinetic simulations can include multiple ion components, and they demonstrate transport interference among impurities, bulk fuels, energy and/or momentum [6].

In addition to transport interference, another attractive feature of turbulence and transport in fusion plasmas is that they can be dynamic. Namely, turbulence and transport can transiently change in magnetized plasmas [7–9]. Examples of such behaviors include, but not limited to, ELMs [10], blobs [11], Sawtooth [12], etc. These phenomena can transiently change the level of turbulent fluctuations and transport. This property appears to be attractive to exhaust harmful components, since transport is enhanced during a limited amount of time. We can minimize the loss of bulk fuel particles and energy in this approach. We need a deep understanding of the origin and the nature of transient behavior of magnetized plasmas to exploit this property.

* Author to whom any correspondence should be addressed.

In the context of dynamic behavior of fusion plasmas, a recent work reports the possibility of a new origin different from those listed above. This is based on the excitation of nonlinear breathers [13] in turbulent fluctuation. A breather is a type of nonlinear wave. Unlike solitons, which stably propagate, breathers introduce transient increase of wave energy. The wave energy accumulates due to modulational instability, and at the nonlinear stage of the evolution, the accumulated energy is spatially redistributed. The overall dynamics looks as if waves are breathing, and leads to the transient change of wave amplitude. Breathers have gathered attention in the context of oceanography, where the excitation of freak/rogue waves is a relevant issue. A model is proposed to explain the excitation of freak waves based on breathers, and this has been confirmed in water tank experiments [14]. Since then, breathers are observed in various systems, such as optical fibers [15], dusty (complex) plasmas [16]. Breathers are also excited from drift waves, which we call as a drift breather [17]. The excitation of drift breathers are confirmed in basic experiments, and transient increase of particle flux is also confirmed in data analysis.

Since the previous work on breather excitation in magnetized plasmas is based on a model with a single ion species, this raises a question whether it is possible or not to excite transient breathers in magnetized plasmas with multiple ion species. The purpose of this work is then to elucidate the dynamic behavior of turbulent plasmas in the presence of impurities. To illustrate this aspect, we develop a simplified fluid model which describes the nonlinear evolution of fluctuations in the presence of multiple ions, or impurities. Based on this model, we can discuss relevant fluctuation excited in the system. As shown later, a similar model to that for 'pure' drift waves can be constructed in the presence of impurities. Underlying wave property is summarized, and impurities modify basic time and spatial scales, such as ion cyclotron frequency, Larmor radius, etc. As a consequence, the group velocity and/or dispersion of wave packet become a function of impurity parameters such as mass, charge, and concentration.

Then the nonlinear dynamics of underlying waves is analyzed based on modulational analysis. Impurity drift waves nonlinearly exert Reynolds stress to drive large scale flows, such as zonal flows [18], streamers [19–22] (radially elongated convective cells). These flows in turn feedback onto the original waves. The nonlinear dynamics of waves with flow coupling is formulated as one dimensional Schrödinger equation (1D NLSE). 1D NLSE is used to describe the nonlinear evolution of dispersive impure drift waves and we found that the excitation of breathers is possible. To excite breathers, the amplitude of underlying waves need to be large enough. The critical amplitude is derived and compared against the case without impurity coupling. Interestingly, we found that within this model the excitation of breathers becomes easier in the presence of impurities. The role of parallel flows is also discussed, and the result indicates that parallel flows may decrease the critical amplitude for exciting breathers. Hence, rotating plasmas with impurities may accompany multiple breathers, and may be very dynamic. We elaborate implications on fusion experiments later.

The remaining of the paper is organized as follows. In section 2, we derive a fluid model for describing low frequency fluctuation dynamics in magnetized plasmas with impurities. Relevant modes are derived and we find that modified drift waves and parallel velocity gradient (PVG) driven instability may arise for these plasmas. Section 3 then describes relevant wave feature predicted from this model. Nonlinear dynamics is formulated in section 4 based on modulational analysis. Section 5 is conclusion and discussion.

2. Model

Here we introduce a reduced fluid model to describe the nonlinear evolution of fluctuations with multi-species ions. For simplicity, we consider electro-static drift wave turbulence with the coupling to impurity. We also use a simplified slab geometry, and toroidicity effect is neglected in this paper. In this sense, the derivation of the model is very similar to that for Hasegawa-Mima model for drift wave turbulence with a single ion. In our model, we assume that electrons, ions, and impurities are all magnetized. In other words, the typical frequency of fluctuations are assumed to be smaller compared to the cyclotron frequency of each particle species. Electrons respond to the electric field perturbation and move rapidly along the magnetic field line. As a consequence, the electron response is assumed to be close to Boltzmannian,

$$\frac{\tilde{n}_e}{\langle n_e\rangle} = \frac{e\tilde{\phi}}{T_e} \tag{1}$$

$\langle n_e\rangle$ is the average electron density, and $\tilde{(\ldots)}$ denotes fluctuation. We note that a finite phase shift is necessary to have instability and electron particle flux. We nevertheless assume the Boltzmann response for simplicity, since our purpose here is to elucidate the nonlinear evolution of fluctuations. The relevance of the phase shift is further discussed later in this work. For ions and impurities, which are magnetized, the perpendicular velocity is calculated as

$$\tilde{v}_{\perp,s} = \frac{c}{B}\hat{z}\times\nabla_\perp\tilde{\phi} - \frac{1}{\omega_{cs}}\frac{\mathrm{d}}{\mathrm{d}t}\frac{c}{B}\nabla_\perp\tilde{\phi}. \tag{2}$$

Here $\hat{z}$ is the direction of the magnetic field, $\omega_{cs} = e_sB/(m_sc)$ is the cyclotron frequency for a particle species s and $\mathrm{d}/\mathrm{d}t = \partial_t + (c/B)\hat{z}\times\nabla_\perp\tilde{\phi}\cdot\nabla_\perp$. The first term is $E\times B$ drift and common to each particle species. The second term is polarization drift and proportional to mass. Hence this effect is more important for ions. The density response is then given by

$$\frac{\mathrm{d}\tilde{n}_s}{\mathrm{d}t} - \frac{c}{B}\frac{\partial\tilde{\phi}}{\partial y}\frac{\partial\langle n_s\rangle}{\partial x} - \frac{1}{\omega_{cs}}\frac{\mathrm{d}}{\mathrm{d}t}\frac{c}{B}\nabla_\perp^2\tilde{\phi} + \langle n_s\rangle\nabla_\parallel\tilde{v}_{\parallel,s} = 0 \tag{3}$$

x is the direction of the inhomogeneity (i.e. the radial direction), y is the poloidal direction. The correspondence between

(x,y) and (r,θ) is understood hereafter. Here finite parallel compression is included. The parallel momentum balance is

$$\frac{\mathrm{d}\tilde{v}_{\parallel,s}}{\mathrm{d}t} - \frac{c}{B}\frac{\partial\tilde{\phi}}{\partial y}\frac{\partial\langle v_{\parallel,s}\rangle}{\partial x} = \frac{Z_s e_s}{m_s}\tilde{E}_{\parallel}. \tag{4}$$

Here ions and impurities are assumed to be cold, and the viscous damping is also neglected. More detailed study on how these parameters impact the excitation of fluctuation is discussed elsewhere. By using the quasi-neutrality condition $\tilde{n}_e = \tilde{n}_i + Z\tilde{n}_Z$ and adding the density evolutions for ions and impurities, the set of equations can be combined to give

$$\left(\frac{\partial}{\partial t} + \frac{c}{B}\hat{z}\times\nabla_\perp\tilde{\phi}\cdot\nabla_\perp\right)\left(1-\bar{\rho}^2\nabla_\perp^2\right)\frac{e\tilde{\phi}}{T_e} + v_{*e}\frac{\partial}{\partial y}\frac{e\tilde{\phi}}{T_e} + \nabla_\parallel\widetilde{v}_\parallel = 0 \tag{5}$$

$$\left(\frac{\partial}{\partial t} + \frac{c}{B}\hat{z}\times\nabla_\perp\tilde{\phi}\cdot\nabla_\perp\right)\widetilde{v}_\parallel - \rho_s c_s\overline{\langle v_\parallel\rangle'}\frac{\partial}{\partial y}\frac{e\tilde{\phi}}{T_e} = -\bar{c}_s^2\nabla_\parallel\frac{e\tilde{\phi}}{T_e}. \tag{6}$$

Here, v_{*e} is the electron diamagnetic velocity, and we defined the effective parallel velocity and the velocity shear as

$$\widetilde{v}_\parallel = \frac{\langle n_i\rangle\tilde{v}_{\parallel,i} + Z\langle n_Z\rangle\tilde{v}_{\parallel,Z}}{\langle n_e\rangle} \tag{7}$$

$$\overline{\langle v_\parallel\rangle'} = \frac{\langle n_i\rangle\langle v_{\parallel,i}\rangle' + Z\langle n_Z\rangle\langle v_{\parallel,Z}\rangle'}{\langle n_e\rangle}. \tag{8}$$

The scale length and the sound speed are also given as

$$\bar{\rho}^2 = \rho_s^2\frac{\langle n_i\rangle + A\langle n_Z\rangle}{\langle n_e\rangle} = \rho_s^2\frac{1+AC}{1+ZC} \tag{9}$$

$$\bar{c}_s^2 = c_s^2\frac{\langle n_i\rangle + \left(Z^2/A\right)\langle n_Z\rangle}{\langle n_e\rangle} = c_s^2\frac{1+\left(Z^2/A\right)C}{1+ZC}. \tag{10}$$

Here $c_s^2 = T_e/m_i$ and $\rho_s = c_s/\omega_{ci}$ are the ion acoustic speed and the ion sound Lamor radius. $\bar{\rho}$ and $\bar{c}_s$ are a typical scale length and a typical sound speed, which include the coupling to impurities. The effect of impurities enters through the concentration $C = n_Z/n_i$, the charge number Z and the mass number $A = m_Z/m_i$.

Though simplified, the reduced model can be used to extract the evolution of fluctuations with impurities. Typical features of underlying modes can be obtained from linear analysis. Fourier analysis of equations (5) and (6) provides the dispersion relation as

$$\left(1+\bar{\rho}^2k_\perp^2\right)\omega^2 - \omega_{*e}\omega - k_\parallel^2\bar{c}_s^2 + k_\parallel c_s\rho_s k_y\overline{\langle v_\parallel\rangle'} = 0 \tag{11}$$

$\omega_{*e} = k_y v_{*e}$ is the electron drift frequency. This can be solved to obtain

$$\omega = \frac{\omega_{*e}}{1+\bar{\rho}^2k_\perp^2}\frac{1\pm\sqrt{D}}{2} \tag{12}$$

where

$$D = 1 + 4\left(1+\bar{\rho}^2k_\perp^2\right)\frac{k_\parallel^2\bar{c}_s^2 - k_\parallel c_s\rho_s k_y\overline{\langle v_\parallel\rangle'}}{\omega_{*e}^2}. \tag{13}$$

We note that the mode can be unstable for large parallel velocity shear. For this to be true, we need to have $k_\parallel k_y\overline{\langle v_\parallel\rangle'} > 0$. This mode is most unstable for $k_\parallel\bar{c}_s = (c_s/\bar{c}_s)\rho_s k_y\overline{\langle v_\parallel\rangle'}/2$ and for this wave number we have

$$D = 1 - \left(1+\bar{\rho}^2k_\perp^2\right)\frac{\overline{\langle v_\parallel\rangle'}^2}{\left(\bar{c}_s/L_{n_e}\right)^2}. \tag{14}$$

When the parallel velocity shear exceeds the critical value, $\overline{\langle v_\parallel\rangle'}^2 > (\bar{c}_s/L_{n_e})^2/(1+\bar{\rho}^2k_\perp^2)$, we have instability. This is called PVG instability [23–28]. PVG can be driven either by the main ion velocity shear or by the impurity velocity shear, and we may call 'pure' PVG and 'impure' respectively [28]. Impurity provides a novel route to control PVG through the effective shear and detailed analysis is currently on-going. Since analysis on PVG with impurity is reported in [28], here we focus on PVG *stable* case. Then relevant fluctuation here is a drift wave with coupling to impurities. This can be directly seen by setting $\overline{\langle v_\parallel\rangle'} \to 0$, which leads to $\omega \to \omega_{*e}/(1+\bar{\rho}^2k_\perp^2)$. Note that the drift wave branch appears from the branch with the positive sign in equation (12). In the rest of the work, we take this mode as a typical wave excited in magnetized plasmas with impurities, analyze their nonlinear evolution, and then discuss the impact of the presence of impurities.

3. Wave properties of impure drift waves

Before starting detailed nonlinear analysis, we briefly summarize relevant wave feature that can be described at the linear level. Indeed it is very important to grasp some of the wave properties, such as propagation at the group velocity, the spread of a wave packet due to dispersion, etc, to understand nonlinear evolution of impure drift waves, as shown later. In order to demonstrate how group velocity and dispersion impact wave dynamics, here we use a Gaussian wave packet as a concrete example. To make the story simple, we consider a one dimensional model, where a physical quantity $f(x,t)$ is written as Fourier integral

$$f(x,t) = \int \mathrm{d}k F(k)\, e^{ikx - i\omega(k)t} + \text{c.c.} \tag{15}$$

Note that this is not a Fourier decomposition in (k,ω) with complex $F(k,\omega)$. Rather, $F(k)$ is real, and all waves are assumed to be in phase at $x=0$, $t=0$. Here the shape of the spectrum is taken as

$$F(k) = \frac{1}{\sqrt{2\pi}\Delta k}\exp\left(-\frac{(k-k_0)^2}{2\Delta k^2}\right). \tag{16}$$

At $t=0$, the spatial distribution is easily calculated as

$$f(x,t=0)=e^{ik_0x}\exp\left(-\frac{\Delta k^2x^2}{2}\right). \tag{17}$$

Thus the wave is localized around the origin $x=0$. At a later time with finite t, we calculate the integral by expanding $\omega(k)\cong\omega_0+(\partial\omega/\partial k)(k-k_0)+(\partial^2\omega/\partial k^2)(k-k_0)^2/2+\ldots$. The integral over k can be then performed to give

$$f(x,t)=e^{ik_0x-i\omega_0t}\times\frac{1}{\sqrt{1+i\frac{\partial^2\omega}{\partial k^2}\Delta k^2t^2}}\exp\left(-\frac{1}{2}\frac{\Delta k^2\left(x-v_gt\right)^2}{1+i\frac{\partial^2\omega}{\partial k^2}\Delta k^2t^2}\right)+\text{c.c.} \tag{18}$$

The peak of the wave packet amplitude propagates at the group velocity $v_g=\partial\omega/\partial k$. As time goes by, the wave packet spatially disperses. The degree of the dispersion is given by $\partial^2\omega/\partial k^2$.

The actual wave dynamics associated with the impure drift wave is two dimensional. The group velocity in each direction (radial and poloidal) is calculated as

$$v_{gx}=\frac{\partial\omega}{\partial k_x}=-\frac{2\bar{\rho}^2k_xk_yv_{*e}}{\left(1+\bar{\rho}^2k_\perp^2\right)^2}\left(\frac{1+\sqrt{D}}{2}+\frac{\left(1+\bar{\rho}^2k_\perp^2\right)\bar{M}^2}{4\sqrt{D}}\right) \tag{19}$$

$$v_{gy}=\frac{\partial\omega}{\partial k_y}=v_{*e}\frac{1+\bar{\rho}^2k_x^2-\bar{\rho}^2k_y^2}{\left(1+\bar{\rho}^2k_\perp^2\right)^2}\frac{1+\sqrt{D}}{2}-\frac{\bar{\rho}^2k_y^2v_{*e}}{2\left(1+\bar{\rho}^2k_\perp^2\right)}\frac{\bar{M}^2}{\sqrt{D}}. \tag{20}$$

where $\bar{M}^2=\overline{\langle v_\parallel\rangle'}^2/(\bar{c}_s/L_{n_e})^2$. Figure 1 describes the dependence of the group velocity on impurity concentration. The value is normalized by the electron drift velocity, v_{*e}. Parameters are chosen as $A=12$ (Carbon), $Z=3$, $\bar{M}=0.1$, $k_x\rho_s=-0.6$, $k_y\rho_s=0.7$. Note that $k_xk_y<0$ is required from the out-going wave boundary condition, $v_{gx}>0$. As we can see, the group velocity tends to decrease as we increase the impurity concentration (except for v_{gx} in the range of $n_z/n_i\lesssim 0.04$). The variation is anisotropic; while v_{gx} has weak dependence on the concentration, the impact of impurity content is more effective for the poloidal propagation.

We can similarly evaluate the degree of wave dispersion. The results are

$$\frac{\partial^2\omega}{\partial k_x^2}=\frac{v_{*e}\bar{\rho}^2k_y}{2\left(1+\bar{\rho}^2k_\perp^2\right)^3}\times\frac{\left(3\bar{\rho}^2k_x^2-1-\bar{\rho}^2k_y^2\right)\left(D+2D^{3/2}+D^2\right)-\bar{\rho}^2k_x^2\left(1+\bar{\rho}^2k_\perp^2\right)^2\bar{M}^4}{D^{3/2}} \tag{21}$$

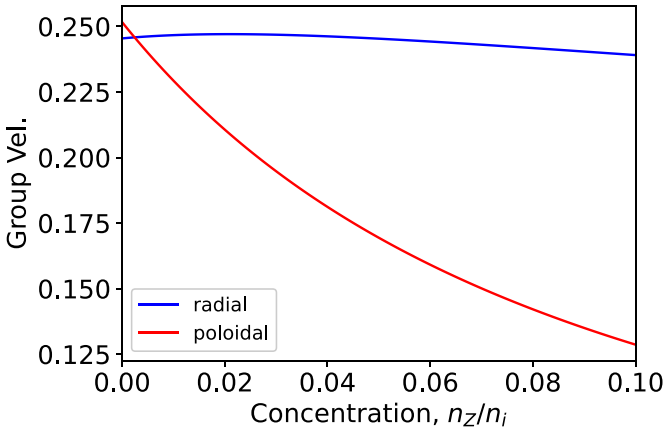

Figure 1. Dependence of group velocity in the radial and poloidal directions on impurity concentration. Here the value is normalized by v_{*e}.

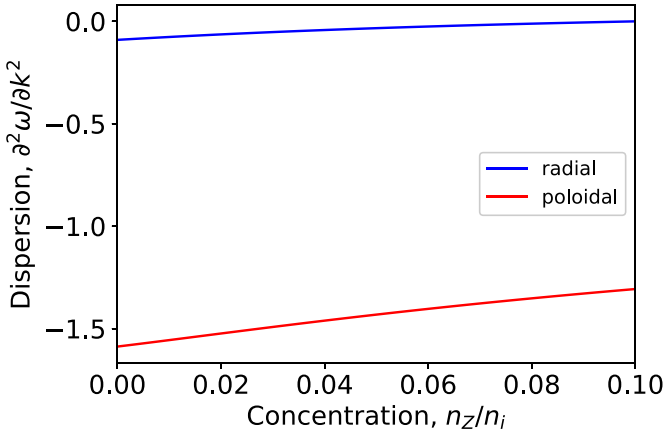

Figure 2. Dispersion of impure drift waves. As the concentration increases, the dispersion becomes weaker. Thus waves become more coherent in the presence of impurities.

$$\frac{\partial^2\omega}{\partial k_y^2}=\frac{v_{*e}\bar{\rho}^2k_y}{\left(1+\bar{\rho}^2k_\perp^2\right)^3}\times\frac{\left(\bar{\rho}^2k_y^2-3-3\bar{\rho}^2k_x^2\right)\left(D+2D^{3/2}+D^2\right)-\bar{\rho}^2k_y^2\left(1+\bar{\rho}^2k_\perp^2\right)^2\bar{M}^4}{D^{3/2}}. \tag{22}$$

Typical behavior is plotted in figure 2. Here the parameters are same as those for figure 1, and the value is normalized by $v_{*e}\rho_s$. We see that poloidal dispersion is stronger than radial dispersion. We also note that the degree of dispersion decreases for both radial and poloidal direction, as we increase the concentration of impurities. Drift waves with certain impurity concentration become more coherent and do not easily disperse especially in the radial direction. As we elaborate later, this helps impure drift waves to be modulationally unstable and to develop into nonlinear breathers. This argument is only based on the wave dispersion and we are still

missing the effect to allow drift waves to spatially condensate. This can be implemented by analyzing the nonlinear evolution and will be treated in the next section.

4. Excitation of impure drift breather

4.1. Formulation

Here we discuss a model to elucidate the nonlinear evolution of impure drift wave packet. As discussed above, the presence of impurities impact the dispersion of the packet. In addition to this, impurities can impact nonlinear evolution. This may be understood by analyzing the interaction of impure drift waves and flows. As is well known, drift waves can nonlinearly interact with each other to pump large scale flows, such as zonal flows and/or streamers. Once excited, flows feedback on the underlying waves. This nonlinear interaction can be formulated by modulational analysis [29–32]. Here we describe relevant ideas and assumptions behind this approach. In this approach, we write the total potential field as $\phi = \tilde{\phi} + \Phi$, where $\tilde{\phi}$ is for underlying fluctuation and Φ is a meso-scale component, represented by convective cells, zonal flows, and/or streamers. The equation for fluctuations, with coupling to the meso-scale field, is then given by

$$\mathcal{L}\frac{e\tilde{\phi}}{T_e} = \mathcal{N}\left(\tilde{\phi}, \Phi, N_e, \bar{V}_\parallel\right). \tag{23}$$

Here $\mathcal{L}$ is an operator defined as

$$\mathcal{L} = \frac{\partial^2}{\partial t^2}\left(1-\bar{\rho}^2\nabla_\perp^2\right) + v_{*e}\partial_t\partial_y + \nabla_\parallel\left(-\bar{c}_s^2\nabla_\parallel + \rho_s c_s\overline{\langle v_\parallel\rangle'}\partial_y\right) \tag{24}$$

$\mathcal{N}$ is a nonlinear term, and this is due to the modulation from the large scale fields Φ, N_e, and $\bar{V}_\parallel$. The nonlinear term is specifically given by

$$\begin{aligned}\mathcal{N} = \frac{\partial}{\partial t}\Bigg(&-\frac{c}{B}\hat{z}\times\nabla_\perp\Phi\cdot\nabla_\perp\left(1-\bar{\rho}^2\nabla_\perp^2\right)\frac{e\tilde{\phi}}{T_e}\\ &-\frac{c}{B}\hat{z}\times\nabla_\perp\tilde{\phi}\cdot\nabla_\perp\frac{N_e}{\langle n_e\rangle}\Bigg) - \nabla_\parallel\Bigg(-\frac{c}{B}\hat{z}\times\nabla_\perp\Phi\cdot\nabla_\perp\widetilde{\bar{v}_\parallel}\\ &-\frac{c}{B}\hat{z}\times\nabla_\perp\tilde{\phi}\cdot\nabla_\perp\bar{V}_\parallel\Bigg).\end{aligned} \tag{25}$$

Here we note that the nonlinear interaction is primarily given by the modulation by the large scale fields. The nonlinear interaction among small scale components is mainly responsible for the evolution of large scale flows, as discussed later. While the interaction among small scales may be also important for the evolution of $\tilde{\phi}$ for the case of broad spectrum, here we neglect the effect and focus on the feedback from large scale flows. The nonlinear coupling modulates the underlying drift waves. This effect can be captured by writing the wave field as

$$\tilde{\phi} = \mathrm{Re}\left(\psi e^{i\mathbf{k}\cdot\mathbf{x}-i\omega t}\right), \tag{26}$$

where ψ is the complex envelope. The envelope is assumed to vary slower compared to the underlying waves, which means

$$\left|\frac{\partial_t\psi}{\psi}\right| \ll \omega, \ \left|\frac{\nabla\psi}{\psi}\right| \ll |\mathbf{k}|. \tag{27}$$

We note that large scale fields also vary with the similar temporal and spatial scales. The disparity in the scales can be implemented by introducing slow variables, such that

$$\nabla \to \frac{\partial}{\partial\mathbf{x}} + \epsilon\frac{\partial}{\partial\mathbf{X}}. \tag{28}$$

Here the lower case $\mathbf{x}$ captures the fast variation associated with fluctuation, and thus $\partial/\partial\mathbf{x}\sim\mathbf{k}$. The variable with the capital letter $\mathbf{X}$ captures the modulation effect. A small parameter ϵ is introduced, and we typically have $e\tilde{\phi}/T_e \sim O(\epsilon)$. We note that envelope and large scale fields are a function of this slow variable. Similarly, the temporal evolution is given by

$$\partial_t \to \partial_t + \epsilon\partial_T + \epsilon^2\partial_\tau. \tag{29}$$

Here the time variation is expanded up to $O(\epsilon^2)$. This is since nontrivial dynamics appears at this order, as shown later.

The dynamics of fluctuations with nonlinear evolution can be systematically described by analyzing the underlying equation order by order. To the lowest order in ϵ, we have

$$\mathcal{L}_0(\omega,\mathbf{k}) = 0. \tag{30}$$

This corresponds to the dispersion relation discussed above. Here underlying waves are impure drift waves. To the next order, we have

$$\left(\frac{\partial\mathcal{L}_0}{\partial\omega}\frac{\partial}{\partial T} - \frac{\partial\mathcal{L}_0}{\partial\mathbf{k}}\cdot\frac{\partial}{\partial\mathbf{X}}\right)\psi = 0. \tag{31}$$

Since $\mathbf{v}_g = -(\partial\mathcal{L}_0/\partial\mathbf{k})/(\partial\mathcal{L}_0/\partial\omega)$ is the group velocity, the dynamics at this order corresponds to the propagation of impure drift wave packet at $\mathbf{v}_g$. This can be eliminated by going to the moving frame. Nontrivial, lowest order nonlinear dynamics is then obtained at the second order as

$$\left(i\frac{\partial\mathcal{L}_0}{\partial\omega}\frac{\partial}{\partial\tau} + \frac{1}{2}\frac{\partial^2\omega}{\partial k_i\partial k_j}\frac{\partial}{\partial X_i}\frac{\partial}{\partial X_j}\frac{\partial\mathcal{L}_0}{\partial\omega}\right)\psi = \mathcal{N}\left(\tilde{\phi},\Phi,N_e,\bar{V}_\parallel\right). \tag{32}$$

Here, the second term in the lefthand side is related to the dispersion of the wave packet discussed above. Thus, up to the nonlinear term in the righthand side, the dynamics of impure drift wave is similar to that of the wave packet, i.e. propagation at the group velocity and spatial dispersion. The nonlinear term introduces new effect for this wave dynamics. The nonlinear term leads to the modulation of the packet.

To make further progress, we need to formulate the evolution of large scale fields. Impure drift waves nonlinearly interact and exert Reynolds stress to pump large scale flows. The evolution of flows can be described by the vorticity evolution,

$$\frac{\partial}{\partial t}\bar{\rho}^2\nabla_\perp^2\frac{e\Phi}{T_e} + \frac{c}{B}\hat{z}\times\nabla_\perp\tilde{\phi}\cdot\nabla_\perp\bar{\rho}^2\nabla_\perp^2\frac{e\tilde{\phi}}{T_e} = 0. \tag{33}$$

Here Φ is the potential for large scale flows and the second term is the nonlinear advection of the vorticity associated with fluctuation (impure drift wave). While the presence of impurities increases the inertia for the flow vorticity evolution, they also enter the inertia for fluctuation vorticity. In total, the impurity effects in inertia, i.e. $\bar{\rho}^2$ cancels in the nonlinear evolution, and the vorticity evolution is given by

$$\frac{\partial}{\partial t}\nabla_\perp^2\frac{e\Phi}{T_e} = -c_s\rho_s\hat{z}\times\nabla_\perp\frac{e\tilde{\phi}}{T_e}\cdot\nabla_\perp\nabla_\perp^2\frac{e\tilde{\phi}}{T_e}. \tag{34}$$

Substituting equation (26) and neglecting terms of order ϵ^3, we have

$$\frac{\partial}{\partial t}\nabla_\perp^2\frac{e\Phi}{T_e} = \frac{\rho_s c_s}{2}\left[k_xk_y\left(\partial_X^2-\partial_Y^2\right)+\left(k_y^2-k_x^2\right)\partial_X\partial_Y\right]\left|\frac{e\psi}{T_e}\right|^2. \tag{35}$$

The large scale flows induce modulation in other physical quantities. In particular, within the model developed here, the flows modulate electron density (which includes main ions and impurities) and the effective parallel flows. Writing these fields as N_e and $\bar{V}_\parallel$, we have

$$\frac{\partial}{\partial t}N_e+\frac{c}{B}\hat{z}\times\nabla_\perp\Phi\cdot\nabla_\perp\langle n_e\rangle = 0 \tag{36}$$

$$\frac{\partial}{\partial t}\bar{V}_\parallel+\frac{c}{B}\hat{z}\times\nabla_\perp\Phi\cdot\nabla_\perp\langle\bar{v}_\parallel\rangle = 0. \tag{37}$$

Note that since the mean quantities are inhomogeneous in the radial (x) direction, these are only finite for streamer flows. Contrarily, modulation of the large scale fields, N_e and $\bar{V}_\parallel$, are small for zonal flows.

The coupled evolution of the wave envelope and large scale fields lead to various interesting phenomena. To extract physics described by the model, we consider a limiting case to simplify the analysis. For this, we consider anisotropic modulation, such as $\partial_X \gg \partial_Y$ or $\partial_X \ll \partial_Y$. In the first case, the radial modulation is stronger compared to the modulation in the poloidal direction. This is often the case for the excitation of zonal flows. The other case corresponds to the stronger poloidal modulation and radial modulation is weak. In this case, radially elongated structures can be excited by the poloidal modulation. A prototypical example for this may be the excitation of radially elongated convective cells, or streamers. In this work, we focus on the latter case, since one motivation for this work is to see whether it is possible or not to degrade confinement for impurity controls. The excitation of zonal flows/GAMs in this framework is also an important topic and will be pursued in the future. Then, by focusing on the case with $\partial_X \ll \partial_Y$, the set of equations can be simplified to give

$$i\frac{\partial}{\partial\tau}\psi+\frac{1}{2}\frac{\partial^2\omega}{\partial k_y^2}\frac{\partial^2}{\partial Y^2}\psi = \left(\frac{\partial\mathcal{L}_0}{\partial\omega}\right)^{-1}\mathcal{N}\left(\tilde{\phi},\Phi,N_e,\bar{V}_\parallel\right) \tag{38}$$

$$-v_{gy}\partial_Y\frac{e\Phi}{T_e} = -\frac{\rho_s c_s}{2}k_xk_y\left|\frac{e\psi}{T_e}\right|^2 \tag{39}$$

$$-v_{gy}\partial_Y N_e = \frac{c}{B}\partial_Y\Phi\langle n_e\rangle' \tag{40}$$

$$-v_{gy}\partial_Y\bar{V}_\parallel = \frac{c}{B}\partial_Y\Phi\langle\bar{v}_\parallel\rangle'. \tag{41}$$

Here the envelope evolution includes the dispersion in the poloidal direction and the nonlinear modulating term. The wave field exerts Reynolds stress to pump large scale flows, or streamers in our case. This radial streamer then modulate the density and the parallel velocity field. These modulating large scale field then feedback onto the underlying wave field, which is included in the nonlinear term in the righthand side. The nonlinear term can be obtained by substituting large scale fields and linear dispersion relations. Then, finally we have a simplified model for the nonlinear evolution of the envelope,

$$i\frac{\partial}{\partial\tau}\psi+\alpha\frac{\partial^2}{\partial Y^2}\psi+\beta|\psi|^2\psi = 0. \tag{42}$$

Here the envelope is normalized as $e\psi/T_e \to \psi$, and the coefficients are

$$\alpha = \frac{1}{2}\frac{\partial^2\omega}{\partial k_y^2} \tag{43}$$

$$\beta = c_sk_x\frac{\rho_s^2k_xk_yc_s}{2v_{gy}}\left(1-\frac{v_{py}}{v_{gy}}\right) \tag{44}$$

$v_{py} = \omega/k_y$ is phase velocity, and the group velocity v_{gy} and the dispersion $\partial^2\omega/\partial k_y^2$ are given above. The coupled evolution of the envelope and large scale fields now reduces to the 1 dimensional Nonlinear Schrödinger equation (1D NLS). While NLS is used analyze quantum physics such as Bose–Einstein condensation and/or quantum turbulence, NLS is also used to analyze classical problems, such as the nonlinear evolution of dispersive waves as discussed here. Indeed, NLS is derived in many contexts, such as surface waves in ocean, light propagating in nonlinear media, various waves in plasmas with nonlinear feedback, etc. Here we have NLS for dispersive impure drift waves with coupling to large scale streamer flows.

NLS contains two parameters, α and β. α is related to the wave dispersion and thus depends on the presence of impurities as discussed above. To elaborate this point, we plot the behavior of α as a function of impurity concentration, for different values of charge state Z. Here carbon is chosen as a typical impurity. As shown in figure 3, as we increase the concentration of impurities, dispersion becomes weak. It becomes easier for wave packets to maintain its spatial patterns. β is related to the coupling to large scale flows and modulation. This coupling introduces nonlinearity in the envelope dynamics. Note that β depends on the factor k_xk_y, which is reminiscent of Reynolds stress. Figure 4 gives the dependence of β on the impurity concentration. As we can see, the presence of impurities leads to stronger coupling to flows. In this model, flow evolution is analyzed in the moving frame of wave packet. As the group velocity decreases for impure plasmas, this leaves more time for waves to exert Reynolds stress to

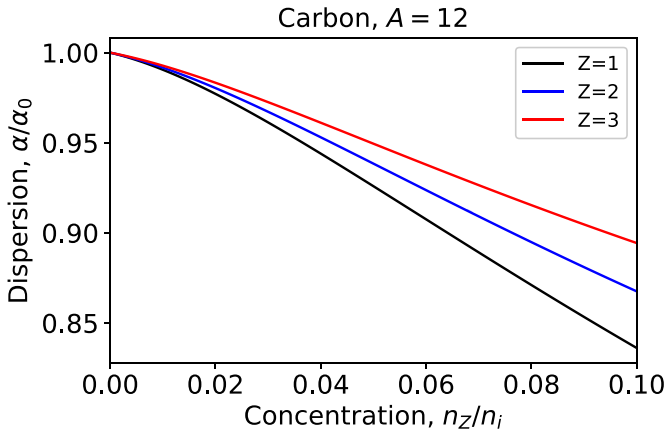

Figure 3. The dependence of dispersion parameter on the impurity concentration. Here α is normalized by α_0, dispersion for a pure plasma. As discussed above, dispersion becomes weaker and thus waves become more coherent in the presence of impurities.

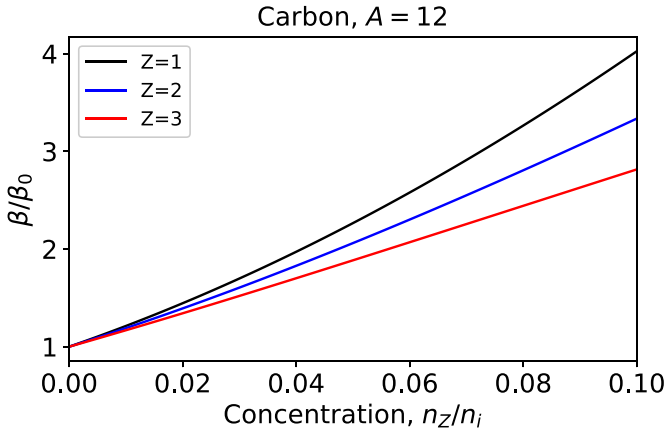

Figure 4. The parameter for nonlinear feedback from flows, β, as a function of impurity concentration. β_0 is the value of β for a 'pure' plasma. As we increase the concentration of impurities, nonlinear feedback becomes stronger. This is since the group velocity decreases, and thus the flow excitation becomes stronger in the presence of impurities.

drive flows. Then flow can be pumped more in the presence of impurities, which leads to the behavior shown in figure 4.

4.2. Nonlinear evolution of envelope with impurities

Here we describe nonlinear dynamics described by 1D NLS. Note that NLS admits a homogenous solution, $\psi = A_0 e^{i\beta A_0^2 t}$. Because of the nonlinear coupling to flows, the frequency of the underlying impure drift wave is shifted. We can perform perturbation analysis for this state. Let $\psi \to (A_0 + \delta A) e^{i\beta A_0^2 t + \delta\theta}$, where δA is amplitude modulation and $\delta\theta$ is phase modulation. Performing Fourier analysis for the modulation, we obtain a dispersion relation

$$\Omega^2 = \alpha^2 q_Y^4 - 2\alpha\beta q_Y^2 A_0^2. \tag{45}$$

Here Ω and q_Y are the frequency and the wave number for the modulation. As we can see, dispersion is stabilizing. When $\alpha\beta > 0$, the perturbation becomes unstable. This leads to the growth of the modulation and pumps large scale flows. In the Fourier space, this corresponds to the spread of energy in the pump wave due to the coupling to large scale modulation. This produces sidebands, which absorb energy from the pump wave. The overall evolution leads to the spread of wave energy in Fourier space. In terms of real space, this leads to the spatial condensation of wave energy. The modulational instability is triggered for large enough wave amplitude. The critical amplitude required for the nonlinear instability is

$$A_0^2 > \frac{\alpha q_Y^2}{2\beta}. \tag{46}$$

The modulation instability is most unstable for $q_Y^2 = (\beta/\alpha)A_0^2$, in which case the growth rate is given by $\Gamma^2 = \beta^2 A_0^4$. These provide typical time and spatial scale for the envelopes.

The nonlinear stage of the modulational growth may be analyzed by solving NLS non-perturbatively. This is indeed possible and NLS admits a nonlinear exact solution,

$$\psi(y,t) = A_0 e^{i\beta A_0^2 \tau} \left(\frac{\sqrt{2}\nu^2 \cosh\left(\beta A_0^2 \sigma\tau\right) + i\sqrt{2}\sigma \sinh\left(\beta A_0^2 \sigma\tau\right)}{\sqrt{2}\cosh\left(\beta A_0^2 \sigma\tau\right) - \sqrt{2-\nu^2}\cos\left(q_Y Y\right)} - 1 \right). \tag{47}$$

Here $\sigma = \nu\sqrt{2-\nu^2}$, $q_Y = \nu\sqrt{\beta A_0^2/\alpha}$ is the wave number of the nonlinear envelope, and ν is a dimensionless parameter that gives spatiotemporal form of the nonlinear wave. We note that $\nu^2 < 2$ is required for this nonlinear solution to exist. This condition can be rewritten as

$$A_0^2 > \frac{\alpha q_Y^2}{2\beta}. \tag{48}$$

This corresponds to the condition for the onset of the modulational instability. Thus, it is very likely that the modulationally unstable wave develops into the nonlinear wave described by this exact solution. The entire dynamics is shown in figure 5. The wave field, which is initially uniform in space, becomes modulationally unstable and the wave energy accumulates in space. This energy is then radiated and distributed in space again. The overall dynamics leads to the transient increase of wave energy.

When the initial wave amplitude is large enough to satisfy equation (48), impure drift waves can develop into nonlinear breathers. It is thus of interest to analyze how impurities influence this critical condition. To see this, we first calculate the critical amplitude for exciting nonlinear breathers as a function of impurity concentration (figure 6). Carbon is chosen as a typical impurity. The result is obtained for different charge state, $Z = 1, 2, 3$. The value is normalized to the critical amplitude without impurities. As we can see, the critical amplitude decreases as impurity concentration increases. If we have more impurities, it becomes easier for impure drift waves to develop into nonlinear breathers. This behavior is consistent with the dependence of parameters for dispersion α and nonlinear coupling β. Impure drift waves becomes less dispersive

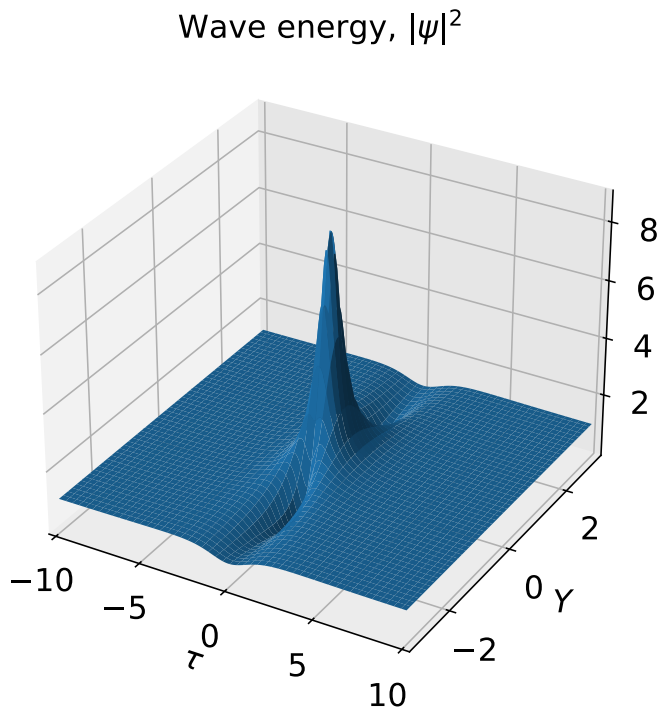

Figure 5. Spatial and temporal pattern of the wave envelope. Parameters are taken as $\nu = 0.1$, $A_0 = \alpha = \beta = 1$ for illustration.

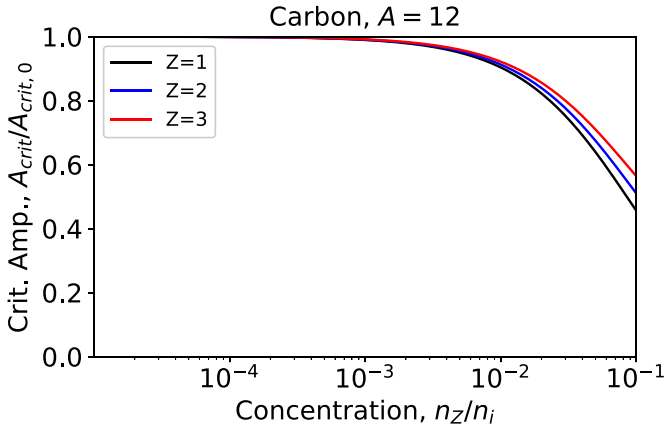

Figure 6. Critical amplitude required for exciting breathers with carbon impurities. Here the value is normalized by the critical amplitude for the case without impurity. The critical amplitude decreases as we increase the impurity concentration. Breathers may be easier to get excited in impure plasmas.

and the flow coupling becomes stronger as impurity concentration increases. These effects act together to make it easier for impure drift waves to develop into nonlinear breathers. We also note that the critical amplitude is higher for higher Z. As we increase Z, the cyclotron frequency goes up, and the effective Larmor radius decreases. This leads to weaker flow coupling and stronger wave dispersion, which are both unfavorable for breather excitation.

While Carbon has been used as a typical impurity in fusion plasmas here, there are other relevant impurities. For example, tungsten impurities gather attention since the introduction of

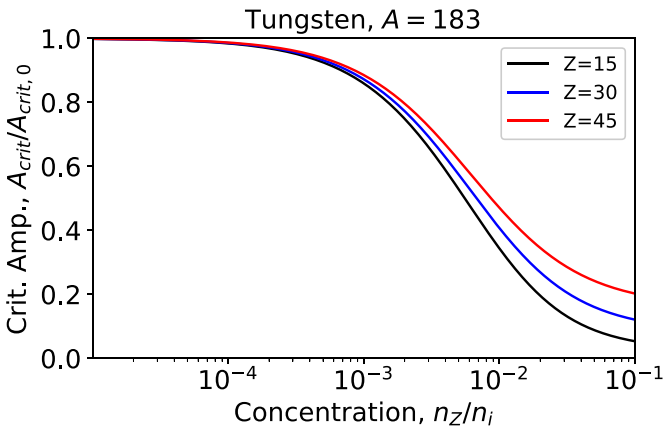

Figure 7. Critical amplitude required for exciting breathers with tungsten impurities. Here the value is normalized by the critical amplitude for the case without impurity. The same trend persists even for tungsten impurities, i.e. breathers are easier to get excited for more impure plasmas. Moreover, this tendency becomes more visible for heavier impurity.

ITER like wall (ILW). In realistic parameter regimes, tungsten Mach number often exceeds unity. However, for simplicity, here we limit our analysis to the regime of Mach number smaller than 1. The parameter scan here may be taken as a preliminary one for more realistic regime. We later elaborate the relevance of the regime of Mach number >1. With this caveat in mind, figure 7 shows the dependence of the critical amplitude for impure drift waves to develop into breathers for the case of tungsten. As we increase tungsten concentration, the critical amplitude becomes lower. The behavior is very similar to the case of Carbon. Furthermore, we note that the critical amplitude becomes even lower for tungsten. Our results indicate that breathers are easier to excite for heavier impurities.

So far we have considered a simplified case without contribution from the parallel flows. However, as discussed for linear mode analysis, the coupling to sheared parallel flows is important and the parallel flows can be a relevant parameter to control fluctuation and possibly nonlinear breathers. Indeed parallel flows can be controlled externally by neutral beam injection etc. Thus it is an interesting and important problem to clarify how these parallel flows interact with breather excitation. The parameters for dispersion α and nonlinear coupling β were already calculated in the presence of parallel shear flows. Then we can evaluate the critical amplitude required for the excitation of breathers as a function of the parallel flow shear. The result is shown in figure 8. Here we have introduced the dimensionless variable $\overline{M} = \overline{\langle v_\parallel \rangle}'/(\bar{c}_s/L_{n_e})$. The critical amplitudes for breather excitation is calculated for both carbon and tungsten. As we can see, the parallel flow shear is effective in regulating breather excitation. In particular, the critical amplitude decreases as the parallel flow shear becomes stronger. This behavior is consistent with previous work on the modulational growth of perpendicular flows [31]. In that work, the modulational growth of flows was found to be amplified by coupling to parallel shear flows. With a finite level of parallel flows, we can have stronger flow excitation and the excitation

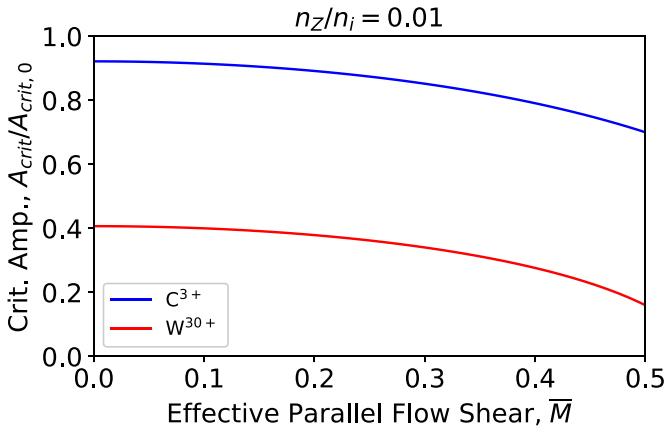

Figure 8. The dependence of critical amplitude on the parallel flow shear. As the shear increases, the critical amplitude is lowered. Thus it may be easier to excite breathers in rotating plasmas.

of breathers becomes easier. Within this model, this dependence originates from the dependence of group velocity on parallel flow shear. In the presence of sheared parallel flows, group velocity decreases. This gives wave packets more time to pump large scale flows. Our result implies that breathers are more easily excited in toroidally rotating plasmas.

Since the parallel flow shear is set by the combination of ion and impurity flows, we have a flexibility in terms of regulating breather excitation. Explicitly, we have

$$\overline{M} = \frac{\langle n_i \rangle \langle v_{\parallel,i} \rangle' + Z \langle n_Z \rangle \langle v_{\parallel,Z} \rangle'}{\langle n_e \rangle (\bar{c}_s / L_{n_e})}. \tag{49}$$

In addition to impurity concentration, the mass number A and the charge Z, we see that impurity flows and ion flows enter as a controlling parameter here. We note that the flow shear is sign dependent. Thus the velocity shear from ions and impurities can add/subtract depending on the profile. This gives room for controlling the effective shear by driving ion and impurity flows independently. For example, when main ions are already rotating with a given flow profile, we may drive impurity flows with a similar flow profile. Then both shear can add up to give a larger value of $\bar{M}$, which makes it easier to excite breathers.

5. Conclusion and discussion

In conclusion, we presented a theory to describe nonlinear dynamics of fluctuations in magnetized plasmas with impurities. In particular, a fluid model was derived to characterize typical fluctuations in such a system. Our model indicates a fluctuation similar to drift waves may be excited, with the typical scale length modified in the presence of impurities. Nonlinear dynamics of impurity drift wave is formulated by modulational analysis. The model includes the nonlinear coupling to flows, and describes the evolution of wave envelope. When the modulation is anisotropic, the model reduces to one dimensional nonlinear Schrödinger equation. Modulational instability is excited when the background wave amplitude becomes large enough, and the nonlinear breather can be excited as a consequence of the nonlinear evolution of this modulational instability. The critical amplitude required for the excitation of nonlinear breathers becomes lower as we increase the impurity concentration. This tendency was more pronounced for heavier impurities. Parallel flow is also important for regulating the excitation of breathers, and breathers are easier to get excited for rotating plasmas.

Based on our results, we speculate that impurities may be self-regulated by turbulent fluctuation. Impurities in toroidal plasmas often accumulate in specific regions, depending on species, collisionality, sources, etc. Then the impurity concentration increases in that region, which lowers the critical amplitude to excite nonlinear breathers. Once breathers are excited, fluctuation amplitude can increase transiently and transport can be enhanced to expel impurities. Of course this is still at the level of theoretical speculation, which needs to be validated in numerical and physical experiments. For this direction, radially elongated flows are observed in toroidal plasmas [33]. The nonlinear evolution of such fluctuation is a prime candidate to excite breathers. We note that the magnetic shear may regulate the excitation of such structures [34]. In this sense, breathers may be easier to observe in plasmas with weak magnetic shear, such as shear-less stellarators, basic linear experiments, etc. Indeed a previous study reports the excitation of breathers and enhancement of turbulent particle flux via data analysis from the linear magnetized plasma experiment, PANTA [17, 35]. A similar experiment and data analysis may be performed with impurities. In addition, a new device called SPEKTRE is under construction and dedicated studies of fluctuations with impurities are planned. This seems an ideal venue to apply our results.

Since this work deals with a simplified model, there is room for further extension. The regime of the Mach number exceeding unity is of interest, given its relevance for heavy impurities such as tungsten. In this direction, the formation of shock structure, the onset of PVG driven turbulence [23, 25, 36–38], along with the excitation of breathers discussed in this work, can be analyzed. These will be elaborated in future studies.

Data availability statement

The data that support the findings of this study are available upon reasonable request from the authors.

Acknowledgments

We thank S Inagaki, H Tsuji, K Terasaka, T Nishizawa for useful discussion. This work is partly supported by the Grants-in-Aid for Scientific Research of JSPS of Japan (JP21H01066,JP22H00243,JP23K20838), the joint research project in RIAM, Kyushu University.

ORCID iD

Y Kosuga https://orcid.org/0000-0002-4075-5542

References

[1] Loarte A *et al* 2007 *Nucl. Fusion* **47** S203
[2] Ida K and Rice J E 2014 *Nucl. Fusion* **54** 045001
[3] Diamond P H *et al* 2013 *Nucl. Fusion* **53** 104019
[4] Garbet X, Garzotti L, Mantica P, Nordman H, Valovic M, Weisen H and ANgioni C 2003 *Phys. Rev. Lett.* **91** 035001
[5] Angioni C, Fable E, Greenwald M, Maslov M, Peeters A G, Takenaga H and Weisen H 2009 *Plasma Phys. Control. Fusion* **51** 124017
[6] Angioni C 2021 *Plasma Phys. Control. Fusion* **63** 073001
[7] Cardozo N J L 1995 *Plasma Phys. Control. Fusion* **37** 799
[8] Ida K *et al* 2015 *Nucl. Fusion* **55** 013022
[9] Ida K, Kobayashi T, Itoh K, Yoshinuma M, Tokuzawa T, Akiyama T, Moon C, Tsuchiya H, Inagaki S and Itoh S -I 2016 *Sci. Rep.* **6** 36217
[10] Zohm H 1996 *Plasma Phys. Control. Fusion* **38** 105
[11] Boedo J A *et al* 2003 *Phys. Plasmas* **10** 1670
[12] von Goeler S, Stodiek W and Sauthoff N 1974 *Phys. Rev. Lett.* **33** 1201
[13] Onorato M, Residori S, Bortolozzo U, Montina A and Arecchi F T 2013 *Phys. Rep.* **528** 47
[14] Chabchoub A, Hoffmann N P and Akhmediev N 2011 *Phys. Rev. Lett.* **106** 204502
[15] Solli D R, Ropers C, Koonath P and Jalali B 2007 *Nature* **450** 1054
[16] Moslem W M, Sabry R, El-Labany S K and Shukla P K 2011 *Phys. Rev.* E **84** 066402
[17] Kosuga Y, Inagaki S and Kawachi Y 2022 *Phys. Plasmas* **29** 122301
[18] Diamond P H, Itoh S I, Itoh K and Hahm T S 2005 *Plasma Phys. Control. Fusion* **47** R35
[19] Nozaki K, Taniuti T and Watanabe K 1979 *J. Phys. Soc. Japan* **46** 991
[20] Yamada T *et al* 2010 *Phys. Rev. Lett.* **105** 225002
[21] Kin F *et al* 2019 *Phys. Plasmas* **26** 042306
[22] Kosuga Y and Hasamada K 2018 *Phys. Plasmas* **25** 100701
[23] Garbet X, Fenzi C, Capes H, Devynck P and Antar G 1999 *Phys. Plasmas* **6** 3955
[24] Garbet X, Sarazin Y, Ghendrih P, Benkadda S, Beyer P, Figarella C and Voitsekhovitch I 2002 *Phys. Plasmas* **9** 3893
[25] Kosuga Y, Itoh S -I and Itoh K 2015 *Plasma Fusion Res.* **10** 3401024
[26] Kosuga Y, Itoh S -I and Itoh K 2017 *Phys. Plasmas* **24** 032304
[27] Guo W, Wang L and Zhuang G 2019 *Nucl. Fusion* **59** 076012
[28] Bourgeois J, Lesur M, Lazaro G C and Kosuga Y 2023 *Open Plasma Science* submitted
[29] Champeaux S and Diamond P H 2001 *Phys. Lett.* A **288** 214
[30] Gürcan O D and Diamond P H 2015 *J. Phys. A: Math. Theor.* **48** 293001
[31] Kosuga Y 2017 *Phys. Plasmas* **24** 122305
[32] Davidson R C 1972 *Methods in Nonlinear Plasma Theory* (Academic)
[33] Cheng J *et al* 2020 *Nucl. Fusion* **60** 046021
[34] Roberts K V and Taylor J B 1965 *Phys. Fluids* **8** 315
[35] Inagaki S *et al* 2016 *Sci. Rep.* **6** 22189
[36] Catto P J, Rosenbluth M N and Liu C S 1973 *Phys. Fluids* **16** 1719
[37] Chapman I T, Brown S, Kemp R and Walkden N R 2012 *Nucl. Fusion* **52** 042005
[38] Wang W X, Ethier S, Ren Y, Kaye S, Chen J, Startsev E, Lu Z and Li Z Q 2015 *Phys. Plasmas* **22** 102509